Journal of Applied Electrochemistry (2006) 36:1223–1229
DOI 10.1007/s10800-006-9182-3

Optimization of CdTe nanofilm formation by electrochemical atomic layer epitaxy (EC-ALE)

V. VENKATASAMY[1], N. JAYARAJU[1], S.M. COX[2], C. THAMBIDURAI[1], U. HAPPEK[2]
and J.L. STICKNEY[1,*]
[1]*Department of Chemistry, University of Georgia, 1001, Cedar street, Athens, GA, 30602, USA*
[2]*Department of Astronomy and Physics, University of Georgia, Athens, GA, USA*
*(*author for correspondence, fax: + 1-706-542-9454; e-mail: stickney@chem.uga.edu)*

Received 27 July 2005; accepted in revised form 10 February 2006

Key words: CdTe, EC-ALE, ellipsometry, EPMA, EQCM, photo voltaics, XRD

Abstract

This paper concerns optimization studies of the growth of cadmium telluride, an important II–VI compound semiconductor, using electrochemical atomic layer epitaxy (EC-ALE). The importance of the potentials used to deposit atomic layers of Cd and Te, as well as the potential used to strip excess Te, were investigated. These potentials were used in a cycle, an EC-ALE cycle, to form deposits one atomic layer at a time, using a sequence of surface limited reactions. The optimal potentials for the CdTe EC-ALE cycle included Cd deposition at -0.65 V, Te deposition at -0.35 V and bulk Te stripping at -0.70 V. The deposits obtained were stoichiometric, with a Te/Cd atomic ratio of 1.01 from electron probe microanalysis (EPMA). Electrochemical quartz crystal microbalance (EQCM) studies of the optimal condition indicated that about a third of the deposited Cd was oxidatively stripped at the potential used to deposit Te. Glancing angle X-ray diffraction studies showed a (111) preferred orientation for the deposit, while room temperature near infrared absorption measurements indicated a direct band gap of 1.5 eV.

1. Introduction

Cadmium telluride, CdTe, is a II–VI compound semiconductor that has found application in the field of photovoltaics [1–5]. Reasons for its use as a photovoltaic include that it possesses a direct bandgap, 1.5 eV, very close to that theoretically calculated to be optimal for solar cells, based on a single absorber, single bandgap configuration. In addition, because of its direct bandgap, it has a very high absorption coefficient.

High quality thin films of CdTe have been achieved with excellent control over stoichiometry and thickness by using high temperature techniques like molecular beam epitaxy (MBE) [6] and metal organic vapor phase epitaxy (MOVPE) [7]. Cadmium telluride has also been obtained by other low temperature techniques like chemical bath deposition (CBD) and electrodeposition [8–13]. Currently, electrodeposition is employed for the fabrication of CdTe films for high efficiency photovoltaic devices [14].

Electrodeposition has advantages such as low or even room temperature deposition, low cost of production and high deposit quality. Cost is the most important factor in making viable photovoltaics for large scale energy conversion. Compound electrodeposition techniques like precipitation [15], co-deposition [16], and EC-ALE [5] have been reviewed in the literature. In general, to achieve the low cost need for general use photovoltaics, co-deposition is probably the only viable electrodeposition methodology.

EC-ALE is a technique for electrodepositing nanofilms, and has been used most extensively to form compound semiconductors. EC-ALE is the electrochemical analog of ALE [17–19] and ALD [20–23], all methods based on the use of surface limited reactions to form deposits with atomic layer control. The advantages of these methodologies are that they can be used to control deposition at the atomic level. The method breaks the deposition process into a sequence of individually controllable steps, thus greatly improving the ability to optimize a process. In some scenarios, they promote epitaxy, as has been found in the case of EC-ALE. However, such processes tend to increase the complexity of the deposition hardware.

In electrochemical studies, surface limited reactions are generally referred to as under potential deposition (UPD) [24–28]. UPD is a phenomenon where one element electrodeposits on another, at a potential prior to (under) the potential at which the first element deposits itself. EC-ALE involves the sequential electrodeposition of atomic layers of elements, to form nanofilms of materials using underpotentials.

Most previous work with EC-ALE has involved electrodeposition of nanofilms of compound semiconductors, including: II–VI compounds such as CdTe, CdS and ZnSe [29–32] as well as some III–V compounds such as GaAs, InAs, and InSb [31–34]. PbSe [35], PbTe and Bi_2Te_3 have also been grown using EC-ALE. Recently, this work has been extended to the formation of metal nanofilms, such as Cu and Pt.

In the authors' group, the formation of CdTe thin films by EC-ALE has been well studied, using a variety of electrochemical cell configurations and geometries, as well as using a variety of cycle programs and solution chemistries [29, 36–38]. The quality of the deposits has improved dramatically from the first studies using a thin layer electrochemical cell (TLE) [39], to the present flow cell design [30]. Early studies were fraught with problems such as poor reproducibility and deposit inhomogeneity. There were also problems with the design of the EC-ALE cycle, and problems deciding on solution composition. Such questions have made it hard to develop and optimize the EC-ALE cycle program. Answers to such questions have become clearer as more studies have been performed on the deposition of CdTe, and other compounds. The cycle program described here has been well optimized by our present standards, for use with the thin layer flow cells used in this study.

As noted above, using EC-ALE to form simple photovoltaics is not economically a wise choice. The quality of a photovoltaic formed using the cycle described here may very well be better then those presently produced using the codeposition method, but the simplicity of codeposition makes it the right choice. This raises the question of what materials are worth depositing via EC-ALE. There are bound to be materials that can only be formed using EC-ALE. However it is more likely that there are structures that can be formed using this method that cannot be formed using another electrodeposition method, or any other method period. For example, when a nanofilm of defined thickness is needed, or the formation of a superlattice, EC-ALE should be considered.

The work presented here has been performed to develop an optimized CdTe cycle, to be combined with one developed for HgTe (to be reported separately) so that superlattices of HgTe and CdTe can be formed and studied. Mer Cad Tel (MCT) is a very important IR detector material ($Hg_XCd_{(1-X)}Te$). It is felt by this group that given EC-ALE programs for both CdTe and HgTe, control over the composition of electrodeposited MCT may be achievable.

This paper presents optimization studies of CdTe deposition by EC-ALE using an automated flow deposition system. The influence of changes in the Cd and Te deposition potentials and the Te stripping potential were varied with the intent of designing a cycle which produces homogeneous and stoichiometric deposits of CdTe, an atomic layer at a time.

2. Experimental

Depositions were performed using a thin layer flow electrodeposition system [5, 40, 41], consisting of pumps, valves, a flow cell and a potentiostat. All components were computer controlled using a LABVIEW program. The flow cell has been described previously [30], with minor design changes to the reference compartment. A Teflon compression fitting was changed to a simple O-ring to hold the reference electrode, providing a better seal. The auxiliary electrode was an ITO glass slide, and the reference was Ag/AgCl (3 M NaCl) (Bioanalytical Systems, Inc., West Lafayette, IN). Substrates consisted of 300 nm thick gold films on glass. The substrates were annealed at 400 °C for 12 h under a vacuum of 10^{-6} Torr, after Au vapor deposition, resulting in a (111) habit.

The solutions used were 0.5 mM $CdSO_4$, pH 5 and 0.2 mM TeO_2, pH 4, and both contained 0.5 M Na_2SO_4. The blank solution contained only the 0.5 M Na_2SO_4, at pH 4. Solution pH was adjusted using H_2SO_4. The water used to make solutions was supplied from a Nanopure water filtration system (Barnstead, Dubuque, IA) attached to the house DI water system. Chemicals were reagent grade or better.

The EC-ALE cycle used to deposit CdTe was as follows: the Cd solution was flushed into the cell for 2 s (40 ml min^{-1}), and then held quiescent for 15 s, all at the chosen Cd deposition potential. Blank solution was then flushed through the cell for 3 s. This was followed by filling the cell with the Te solution for 2 s, and holding quiescent for 15 s for deposition. The cycle was then completed by flushing with blank solution for 3 s. This cycle was repeated 100 times for each experiment.

Deposit thickness was monitored using a single wavelength ellipsometer (Sentech SE 400). A Scintag PAD-V diffractometer with CuK_α radiation ($\lambda = 1.5418$ A), was used to obtain glancing angle X-ray diffraction patterns. Electron probe microanalysis (EPMA) was run on a Joel 8600 wavelength dispersive scanning electron microprobe. Glancing angle absorption measurements were performed, using pi-polarized radiation at a glancing angle of 85 degrees using a 300 W, ozone-free Xe lamp and a monochromator (1/4 M Cornerstone, Spectra Physics).

Optimal deposition conditions were studied using a flow cell electrochemical quartz crystal microbalance (EQCM). A 9 MHz AT-cut quartz crystal (Seiko EG&G) was used, where both sides were coated with circular Au electrodes (ca. 0.2 cm^2, 5 mm in diameter). The electrodes were formed with 50 nm of Ti, followed by 300 nm of sputtered Au. Calibration of the EQCM was carried out using Ag electrodeposition combined with cyclic voltammetry.

3. Results and discussions

The deposition potentials for Cd and Te used in the initial EC-ALE cycle were obtained from cyclic voltammetry, however, these were simple approximations, given that the deposits were formed on Au, not a CdTe surface. The voltammetric behavior of the gold on glass substrates in the blank solution is shown in Figure 1. The Te scan (Figure 2) was started at 0.95 V in the cathodic direction. Three distinct reduction peaks were observed at − 0.35, − 0.10 and 0.28 V, corresponding to the bulk, upd (I) and upd (II), respectively. Further scanning in the cathodic direction resulted in hydrogen evolution below − 0.80 V, as well as the reduction of some bulk Te to a telluride species such as HTe^-. During subsequent anodic scans, peaks at − 0.75, 0.42 and 0.55 V were evident, corresponding to oxidation of HTe^- to Te, and stripping of bulk and upd Te, to $HTeO_2^+$, respectively.

Figure 3 is the cyclic voltammogram for gold on glass in 0.5 mM Cd^{+2}, pH 5 solution. The scan started at 0.55 V in the cathodic direction, showed a reduction shoulder around − 0.05 V, corresponding to Cd^{2+} upd on gold. Bulk Cd deposition occurred at potentials negative of − 0.80 V, and its stripping can be seen in the subsequent oxidative scan, in a peak at − 0.55 V. Besides upd, it is well known that Cd forms an alloy with Au, and the extra current evident in both the reductive and oxidative scans can be ascribed to alloy formation and its subsequent stripping. Cd upd stripped near − 0.15 V.

Potentials of − 0.55 V for Cd and − 0.40 V for Te were chosen, based on the voltammetry. The cycle included a 2 s Cd^{2+} solution rinse followed by 15 s deposition under static conditions (no flow) at − 0.55 V. The cell was then rinsed with blank solution for 3 s at the same potential, followed by a 3 s $HTeO_2^+$ solution rinse and 15 s deposition under static condition at − 0.40 V. The blank solution was again used to flush the $HTeO_2^+$ solution from the cell, for 3 s, at the same potential used for Te deposition.

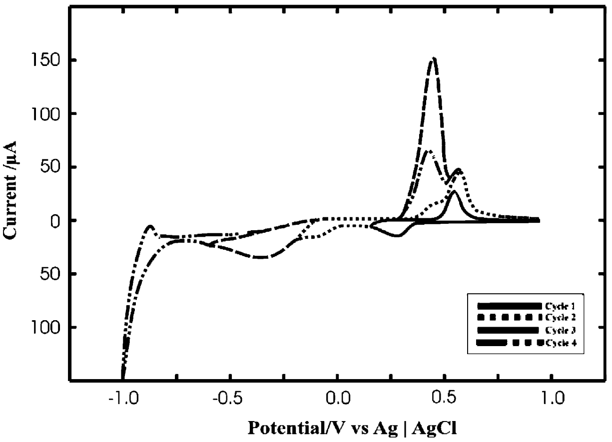

Fig. 2. Cyclic voltammogram of Au electrode in 0.2 mM $HTeO_2^+$, pH 4, (electrode area: 4 cm^2,scan rate: 5 mV s^{-1}).

Previous studies of Te deposition and CdTe formation, using EC-ALE [42], suggested that Te electrodeposition is kinetically slow. In the cyclic voltammetry (Figure 2), no Te deposits were formed at an underpotential, only at overpotentials. However, from the voltammetry for Te deposition (Figure 2), the initial deposition peaks are clearly not the result of a diffusion limited process, but appear to be surface limited reactions. It has been concluded by this group that surface limited deposits of Te are stable on Au, but the kinetics for their deposition are so slow that they do not occur at underpotentials on the experimental time scale, appearing only at overpotentials in the voltammetry. If they are formed at an overpotential, then by definition, bulk Te is stable as well. Hence, formation of just the surface limited amounts of Te becomes problematic. However, the surfaces limited reactions are significantly faster than the bulk deposition reactions. Thus by using short deposition times, the surface limited reactions predominate, but will contain some minimal amount of bulk Te.

A solution to this problem has been to electrochemically reduce the Te deposit in a blank solution, at a fairly negative potential. Under these conditions, bulk

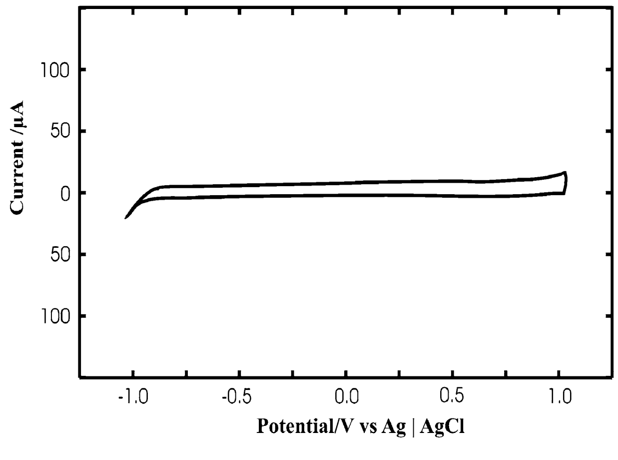

Fig. 1. Cyclic voltammogram of Au electrode in 0.5 M Na_2SO_4, pH 4, (electrode area: 4 cm^2,scan rate: 5 mV s^{-1}).

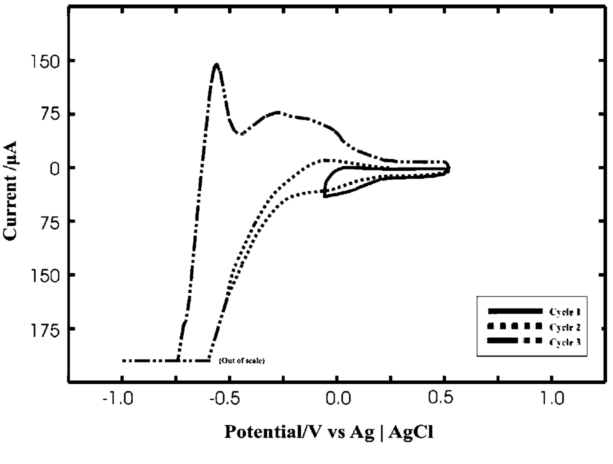

Fig. 3. Cyclic voltammogram of Au electrode in 0.5 mM Cd^{2+}, pH 5, (electrode area: 4 cm^2,scan rate: 5 mV s^{-1}).

Te is reduced to a telluride species, probably HTe^-, which then diffuses away. Te stabilized by bonding to the substrate remains, while the bulk is removed [30]. Thus, to circumvent the problem of traces of bulk Te a reduction step in blank has been inserted after the Te deposition step. Blank solution was rinsed for 3 s at a potential of −0.88 V after the previous blank rinse step.

These steps constituted the initial EC-ALE cycle for CdTe deposition used in the present studies. The resulting CdTe deposit was patchy, inhomogeneous and showed a gradient across the surface. Visual inspection, optical microscopy, and ellipsometric measurements, gave a thicker deposit towards the outlet, with increased roughness there.

At present, deposit quality is gauged by the homogeneity over the deposit surface by optical microscopy, the thickness from ellipsometry, the stoichiometry from EPMA, and the structure from the XRD pattern. As these films are so thin, less then 100 nm, and of a direct band gap material, the color of a deposit is a direct indication of thickness. In addition, significant deposit roughening can be identified by microscopy, and diffuse scattering, scattering of some reflected light. Color changes, as well as scattering can be observed with the eye in many cases.

The need to modify this initial cycle was evident by the variation in color across the deposit. In general, if the deposit shows a gradient in color from the inlet to the outlet, the cycle is not completely controlled by surface limited deposition, as expected. That is, some step(s) in the process probably results in transport controlled deposition. The cycle must be modified to better optimize the process.

From previous work on the EC-ALE formation of CdTe it appears that the reduction of excess bulk Te, the Te stripping step, requires a significant amount of time [42]. Hence, the first change was to increase the time for stripping to 10 s and performing it without solution flow. This was then followed by a blank rinse at the same potential for 1 s, to flush resulting HTe^- species from the cell. The result was greatly improved homogeneity in the deposit. It appears that when the stripping step was performed for a short time with solution flowing, the products of the reduction step, telluride species, may have redeposited further down the substrate, resulting in less at the entrance, where blank entered the cell, and more at the outlet.

With the above change to the stripping step, studies of the potential dependence of the cycle were pursued. First, to determine the optimal deposition potential for Te, a series of experiments were performed where the Te deposition potential was varied from −0.25 V to −0.55 V, while maintaining the Cd deposition potential at −0.65 V and the Te stripping potential at −0.70V (Figure 4). Optical microscopy and EPMA were performed on each of the deposits to determine the homogeneity and stoichiometry respectively. Based on the homogeneity of the deposits and the stoichiometry, it was inferred that the ideal deposition potential for Te was −0.35 V.

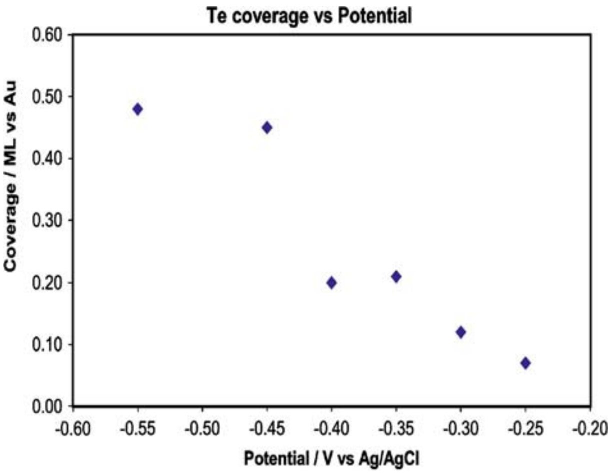

Fig. 4. Effect of Te deposition potential, (Cd deposition potential: −0.65 V; Te stripping potential: −0.70 V).

The potential of −0.35 V was well below the first surface limited peak in Figure 2, but close to the potential observed for the second peak. Figure 4 shows a 50 mV plateau near −0.35 V, consistent with surface limited deposition as opposed to potential controlled deposition, consistent with the improved homogeneity and stoichiometry observed in the deposits. To more negative potentials, the coverage for Te increased rapidly, as bulk deposition becomes more important, while above −0.35 V the coverage dropped, as it was insufficient to deposit a Te atomic layer.

As noted above, the stripping step was required as Te deposition took place negative of the formal potential for the reduction of $HTeO_2^+$ (0.65 V negative of the formal potential), and some bulk was deposit along with the Te atomic layer. A series of experiments was thus performed where the deposition potentials of Cd and Te were held constant at −0.65 V and −0.35 V, respectively, and the Te stripping potential was varied from −0.55 V to −0.80 V (Figure 5). Deposit homogeneity and thickness were again monitored. Deposit thickness

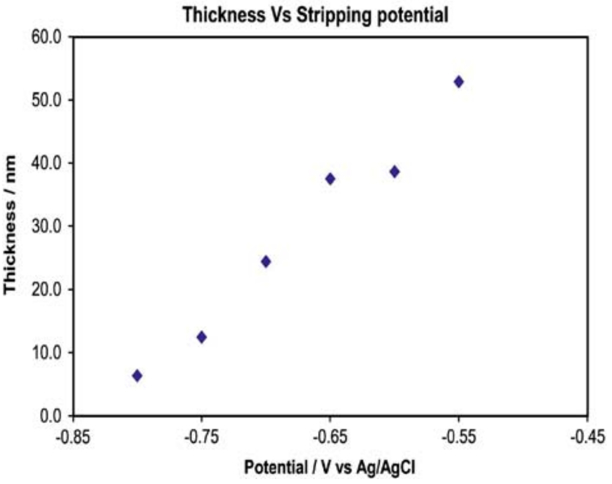

Fig. 5. Effect of Te stripping potential, (Cd deposition potential: −0.65 V; Te deposition potential: −0.35 V).

was observed to decrease as the potential was shifted negatively, as expected, since more Te would be reduced from the surface. In addition, deposit homogeneity decreased at the more negative potentials. Figure 5 suggests that all Te was stripped at sufficiently negative potentials. Similar studies with stripping of Se in the formation of CdSe have shown that all Se can be stripped at sufficiently negative potentials [42]. Based on the deposit stoichiometry data from EPMA, and ellipsometric observations of the deposit thickness and homogeneity, −0.70 V was picked as the reductive stripping potential for the cycle.

To optimize Cd deposition, experiments were performed where the Cd deposition potential was varied between −0.30 V and −0.85 V, keeping all other parameters constant (Figure 6). The best Cd deposition potential appeared to be −0.65 V, where a plateau was evident in the graph. EPMA results indicated potentials below −0.75 V resulted in Cd rich deposits, while those above −0.60 V were Te rich (Figure 7). The Cd coverage took off at potentials below the formal potential for Cd, −0.8V, resulting in excess of 6 ML per cycle, consistent with deposition of bulk Cd.

After the studies described above of the potentials for Cd and Te deposition and the Te stripping potential, the following cycle was devised (Figure 8): Cd^{2+} solution was rinsed for 2 s at −0.65 V, and held for 15 s for deposition. The cell was then flushed with blank for 3 s at −0.65 V. Te solution was then flushed through the cell for 2 s, and held for 15 s at −0.35 V, followed by a blank rinse at −0.35 V for 3 s. The potential was then shifted to −0.70 V for 10 s under static conditions. Finally, the cell was flushed with blank solution at the same potential for 1 s, to remove all HTe^- species form the cell.

The coverages of Cd and Te, from coulometry, for deposits formed with the above cycle were 0.69 and 0.21 ML, respectively, where a monolayer (ML) is defined as one adsorbate atom for every gold surface atom. From previous studies on CdSe, it was found that the formation of one CdSe bi-layer from the (111) plane of zinc blende CdSe would require 0.44 ML of Cd and 0.44 ML of Se [43]. Thus, as a first approximation, similar coverages are expected of Cd and Te in a (111) layer of CdTe. As will be shown below, the predominant orientation for the CdTe deposit, from XRD, was (111). Clearly, the coverages measured here from coulometry are far from those expected for a stoichiometric CdTe deposit, however, EPMA suggests that these deposits are stoichiometric.

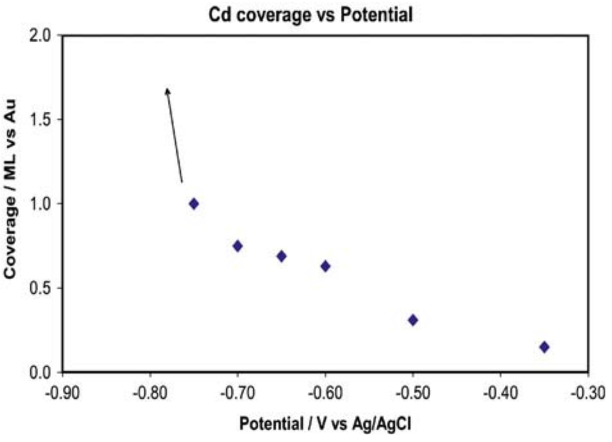

Fig. 6. Effect of Cd deposition potential, (Te deposition potential: −0.35 V; Te stripping potential: −0.70 V).

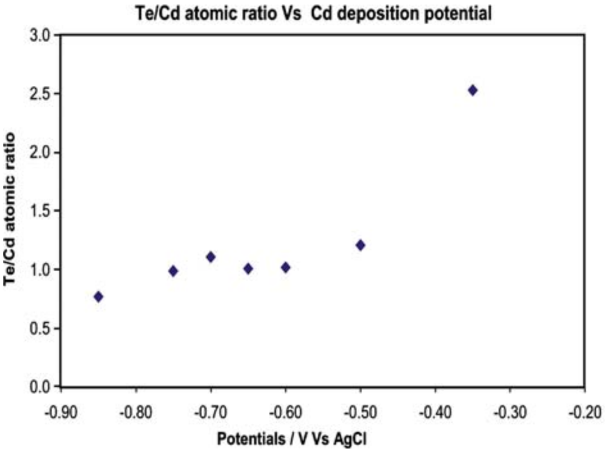

Fig. 7. Effect of Cd deposition potential on the deposit stoichiometry.

In order to better understand the deposition process, and this disparity between charge and stoichiometry, an EQCM (Electrochemical quartz crystal microbalance) study was performed using a similar deposition program. The program did, however, differ as experience has shown that the EQCM flow cell works best if solution is continuously flowed through the cell, but at a much slower flow rate (6 ml min^{-1}). From Figure 9, it is evident, from coulometry, that the Cd coverage was significantly greater than that for Te. It is also clear, that some Cd was oxidatively stripped when the potential was switched from the −0.65 V used to deposit the Cd,

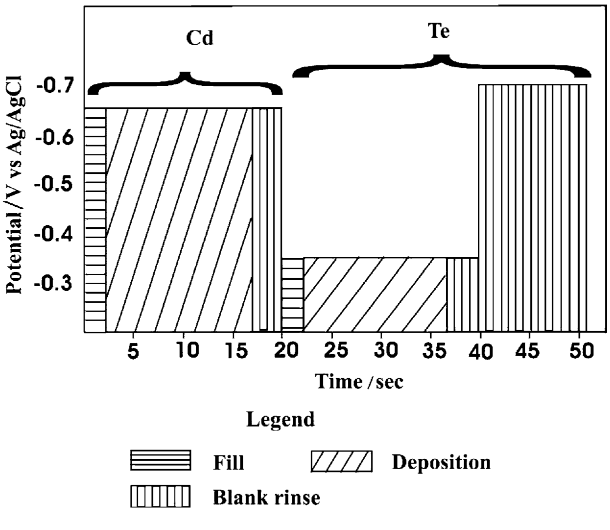

Fig. 8. Optimal deposition program.

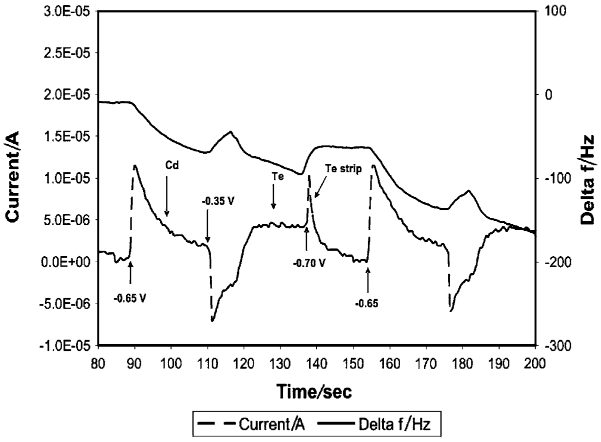

Fig. 9. Current-time profile during CdTe deposition using optimal deposition program by EQCM.

to -0.35V, used to deposit Te. This was evident from both the presence of oxidative current after the potential shift and the mass loss. This is understandable, given the reversibility of Cd deposition, the large positive step in potential and loss of the activity of Cd^{2+} from the solution. The Cd loss was around 0.24 ML, based on coulometry, suggesting a net Cd coverage of around 0.45 ML, about what was expected.

However, measurements from ellipsometry, suggest that the deposit was only 24.4 nm thick, while a 100 cycle deposit of CdTe is expected to be 37.4 nm, based on staking (111) planes of zinc blende. As the deposit was only 24.4 nm thick, instead of 37.4 nm, it is expected that each atomic layer should correspond to a coverage of 0.29 ML in stead of the model of 0.44 ML, as previously suggested. So even taking into account the loss of Cd by oxidation, resulting in a coverage of 0.45 ML, as discussed above, this is still too much Cd to account for a 24.4 nm thick stoichiometric layer of CdTe. In addition, the thickness of the Te layers from coulometry was only 0.21 ML, instead of the 0.29 ML suggested from ellipsometry.

One of the problems with coulometry is that it measures the net current, not the absolute current for a given reaction. From Figure 9 it is evident that the initial deposition current for Te is lower than expected and it may very well be that some Cd was oxidized while Te was initially deposited. If the difference in coverage is taken between what was measured for Cd deposition from coulometry, 0.45 ML, and what was actually realized, 0.29 ML. Based on a stoichiometric layer only 24.4 nm thick, 0.16 ML of Cd is missing each cycle. In the case of Te, a coverage of 0.21 ML was measured from coulometry, and a coverage of 0.29 ML was realized based on stoichiometry and ellipsometry, or a difference of 0.08 ML. Cd oxidation is a two electron process, while that for Te deposition from a tellurite species is a four electron process, so the coverage of Te that would result from the electrons from 0.16 ML of Cd oxidation would be half, or would result in the deposition of an extra 0.08 ML of Te. These numbers suggest that the extra Cd was oxidized by reducing tellurite to Te, resulting in the observed 24.4 nm thick stoichiometric CdTe deposit.

Glancing angle X-ray diffraction was run with an incident angle of 1° from the sample plane, in order to maximize thin film sensitivity (Figure 10). Figure 10 shows the diffraction pattern of a 200 cycle deposit of CdTe, which displays peaks consistent with a zinc blende deposit of CdTe. The relative sizes of the peak indicated a strong (111) preferred orientation. Room temperature absorption measurements of the ideal deposit indicated a direct bandgap of 1.50 eV (Figure 11), consistent with literature values for CdTe.

4. Conclusion

The dependence of nanofilms of CdTe grown using EC-ALE on the deposition potentials used for Cd and Te, as well as that used for a reductive Te stripping step, has been reported. The optimal deposition cycle devised

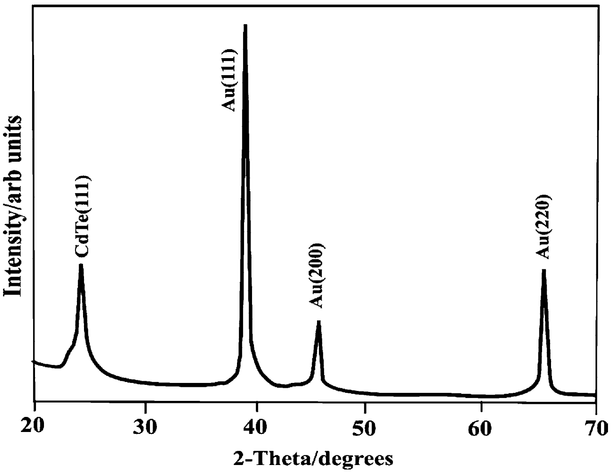

Fig. 10. XRD diffraction pattern of 200 cycle CdTe thin film.

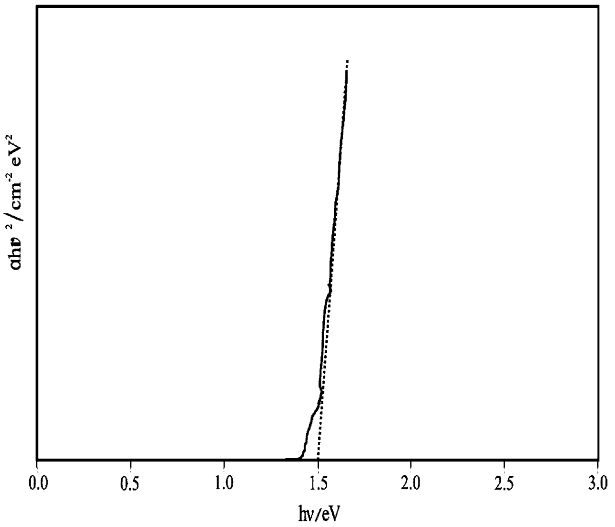

Fig. 11. Absorption spectrum of 200 cycle CdTe thin film.

included deposition of Cd at − 0.65 V, deposition of Te at − 0.35 V and stripping of excess Te at − 0.70 V. The resulting 100 cycle deposit was only 24.4 nm thick, less than that expected from the ideal model of one compound monolayer for each cycle, but the deposit was stoichometric, and showed a strong preferential (111) orientation. The absorption spectrum for this deposit suggested a direct band gap of 1.50 eV, consistent with the literature. Studies using an EQCM flow cell helped in understanding disparities between measured coulometric coverages for Cd and Te, and the resulting stoichiometry and deposit thickness. It appears that some of the Cd each cycle was oxidatively stripped upon switching the potential from the Cd deposition potential of − 0.65V to that for Te deposition, − 0.35V. In addition, it appears that some Cd was exchanged for Te. However, the net result was a high quality nanodeposit of stoichiometric CdTe.

Acknowledgement

The authors acknowledge the support of NSF divisions of Material Science and Chemistry.

References

1. S.A. Gamboa, H. Nguyen-Cong, P. Chartier, P.J. Sebastian, M.E. Calixto and M.A. Rivera, *Sol. Energy Mater.* **55** (1998) 95.
2. N.W. Duffy, L.M. Peter, R.L. Wang, D.W. Lane and K.D. Rogers, *Electrochim. Acta.* **45** (2000) 3355.
3. L.M. Peter and R.L. Wang, *Electrochem. Commun.* **1** (1999) 554.
4. J. Touskova, D. Kindl and J. Tousek, *Thin Solid Films.* **293** (1997) 272.
5. J.L. Stickney, in Electroanalytical Chemistry, Vol. 21 (Marcel Dekker, New York, 1999), 75 pp.
6. A.T.S. Wee, Z.C. Feng, H.H. Hng, K.L. Tran, R.F.C. Farrow and W.J. Choyke, *J. Phys. Chem.: Condens. Matter.* **7** (1995) 4359.
7. K. Maruyama, H. Nishino, T. Okamoto, S. Murakami, T. Saito, Y. Nishijima, M. Uchikoshi, M. Nagashima and H. Wada, *J. Electron. Mater.* **25** (1996) 1353.
8. D. Elwell, *J. Cryst. Growth.* **52** (1981) 741.
9. G.F. Fulop and R.M. Taylor, *Ann. Rev. Mater. Sci.* **15** (1985) 197.
10. B.W. Gregory and J.L. Stickney, *J. Electroanal. Chem.* **300** (1991) 543.
11. K. Rajeshwar, *Adv. Mater.* **4** (1992) 23.
12. G. Fulop, M. Doty, P. Meyers, J. Betz and C.H. Liu, *Appl. Phys. Lett.* **40** (1982) 327.
13. R.K. Pandey, G. Razzini and L.P. Bicelli, *Solar Energy Mater.* **26** (1992) 285.
14. J.M. Woodcock, A.K. Turner, M.E. Ozsan and J.G. Summers, *Thin film solar cells based on electrodeposited CdTe*, presented at the IEEE Photovoltaic specialists, 1991.
15. D. Ham, K.K. Mishra, A. Weiss and K. Rajeshwar, *Chem. Mater.* **1** (1989) 619.
16. F.A. Kroger, *J. Electrochem. Soc.* **125** (1978) 2028.
17. S. Bedair, *Atomic Layer Epitaxy* (Elsevier, Amsterdam, 1993).
18. T.F. Kuech, P.D. Dapkus and Y. Aoyagi, Materials Research Society, Vol. 222 (Pittsburgh, 1991), 360 pp.
19. H. Colin, L. Goodman and M.V. Pessa, *J. Appl. Phys.* **60** (1986) R65.
20. M. Leskela and M. Ritala, *Thin Solid Films.* **409** (2002) 138.
21. E.B. Yousfi, B. Weinberger, F. Donsanti, P. Cowache and D. Lincot, *Thin Solid Films.* **387** (2001) 29.
22. V. Sammelselg, A. Rosental, A. Tarre, L. Niinisto, K. Heiskanen, K. Ilmonen, L.-S. Johansson and T. Uustare, *Appl. Surf. Sci.* **134** (1998) 78.
23. M. Ylilammi, *Thin Solid Films.* **279** (1996) 124.
24. D.M. Kolb, M. Przasnyski and H. Gerisher, *J. Electroanal. Chem.* **54** (1974) 25.
25. D.M. Kolb, in Advances in Electrochemistry and Electrochemical Engineering, Vol. 11 (John Wiley, New York, 1978), 125 pp.
26. K. Juttner and W.J. Lorenz, *Z. Phys. Chem. N. F.* **122** (1980) 163.
27. A.T. Hubbard, V.K.F. Chia, D.G. Frank, J.Y. Katekaru, S.D. Rosasco, G.N. Salaita, B.C. Schardt, D. Song, M.P. Soriaga, D.A. Stern, J.L. Stickney, J.H. White, K.L. Vieira, A. Wieckowski and D.C. Zapien, New Dimensions in Chemical Analysis (Texas A & M University Press, College Station, Texas, 1985), 135 pp.
28. A.A. Gewirth and B.K. Niece, *Chem. Rev.* **97** (1997) 1129.
29. L.P. Colletti and J.L. Stickney, *J. Electrochem. Soc.* **145** (1998) 3594.
30. B.H. Flowers Jr., T.L. Wade, J.W. Garvey, M. Lay, U. Happek and J.L. Stickney, *J. Electroanal. Chem.* **524–525** (2002) 273.
31. T.L. Wade, B.H. Flowers Jr., U Happek and J.L. Stickney, *Formation of II–VI and III–V compound semiconductors by electrochemical ALE*, presented at the National Meeting of the Electrochemical Society, Spring, Seattle, Washington, 1999.
32. T.L. Wade, B.H. Flowers Jr., R. Vaidyanathan, K. Mathe, C.B. Maddox, U. Happek and J.L. Stickney, *Electrochemical Atomic Layer Eptitaxy: Electrodeposition of III–V and II–VI Compounds*, presented at the Materials Research Society, 2000 (unpublished).
33. T.L. Wade, R. Vaidyanathan, U. Happek and J.L. Stickney, *J. Electroanal. Chem.* **500** (2001) 322.
34. T.L. Wade, L.C. Ward and J.L. Stickney, *Chem. Mater.* (1999).
35. R. Vaidyanathan, U. Happek and J.L. Stickney, *Electrochim. Acta.* **49** (2004) 1321.
36. B.W. Gregory, M.L. Norton and J.L. Stickney, *J. Electroanal. Chem.* **293** (1990) 85.
37. B.W. Gregory, D.W. Suggs and J.L. Stickney, *J. Electrochem. Soc.* **138** (1991) 1279.
38. D.W. Suggs, I. Villegas, B.W. Gregory and J.L. Stickney, *Mat. Res. Soc. Symp. Proc.* **222** (1991) 283.
39. D.W. Suggs, B.W. Gregory and J.L. Stickney, *J. Electrochem. Soc.* **138** (1991) 1279.
40. T.L. Wade, TA Sorenson and J. L. Stickney, in Interfacial Electrochemistry, Marcel Dekker (New York, 1999), 757 pp.
41. T. L. Wade, B. H. Flowers Jr., K. Varazo, M. Lay, U. Happek and J. L. Stickney, *Morphology control in the formation of compound semiconductors using electrochemical atomic layer epitaxy (EC-ALE)* (presented at the Electrochemical Society National Meeting, Washington DC, 2001).
42. L.P. Colletti, B.H. Flowers and J.L. Stickney, *J. Electrochem. Soc.* (1997).
43. T.E. Lister and J.L. Stickney, *Appl. Surf. Sci.* **107** (1996) 153.